Supporting Information

Bertrand et al. 10.1073/pnas.1014235108

SI Materials and Methods

Synteny Conservation Analysis. Conserved syntenic regions in the genomes of *Monodelphis domestica*, *Canis familiaris*, *Gallus gallus*, *Xenopus tropicalis*, and *Tetraodon nigroviridis*, which are available in the Ensembl database (http://www.ensembl.org/index.html), and of *Branchiostoma floridae*, which is available at the US Department of Energy Joint Genome Institute (JGI) Web site (http://genome.jgi-psf.org/Brafl1/Brafl1.home.html), were obtained with CASSIOPE (9). When no statistically significant conserved regions containing an FGF gene were found in amphioxus, we searched its genome for orthologs of the genes that were found as part of the conserved regions in at least two vertebrates. Phylogenetic analyses to verify the orthology of each gene within the conserved regions were performed using RaxML version 7.0.4 with the WAG + G + I model, 100 bootstrap replicates, and the rapid bootstrapping algorithm (10). All the accession numbers for genes found in the conserved syntenic regions are given in Table S2.

Immunostaining. Embryos were fixed in 4% (wt/vol) paraformaldehyde as for in situ hybridization but were thereafter kept in PBS + 0.1% Tween 20 at 4° C until use. Three 10-minute washes in PBS + 0.1% Triton X100 were performed, followed by a 1-h incubation in PBS + 1% Triton X100. Embryos were blocked in PBS + 0.1% Triton X100 + 5% (vol/vol) sheep serum + 0.2% BSA for several hours. They were then incubated in blocking solution with antibodies diluted at a ratio of 1/250 [monoclonal antiacetylated-tubulin produced in mouse (T7451; Sigma) and antiphospho-histone H3 (Ser10) (06-570; Millipore)] overnight at 4° C. They were subsequently washed six times for 1 h in PBS + 0.1% Triton X100 and blocked again for several hours. They were then incubated overnight at 4° C in the blocking solution containing secondary antibodies coupled to FITC or Texas Red at a ratio of 1/250. Embryos were then washed three times for 10 min in PBS + 0.1% Tween 20 and mounted in glycerol with 2.5% DABCO (Sigma) for photographs.

Pharmacological Treatments. SU5402 and U0126 were dissolved at 10^{-2} M in DMSO. A range of concentrations, ranging from 10 to 250 μM, was tested. At 10 μM, there is no effect of SU5402 treatment, whereas at >100 μM, development is completely arrested. The highest concentration at which we observe a specific effect is 50 μM, and at this dose, we observe a complete loss of the expression of two orthologs of vertebrate FGF signaling target genes: Dusp6/7/9 and ER81/Erm/Pea3 (Fig. S8). We therefore subsequently performed our experiments using 50 μM SU5402. For U0126, the effect on embryogenesis is specific between 10 and 25 μM; therefore, we used 25 μM except when specified otherwise in the text.

Sections. Sections ranging from 1 to 1.5 μM in thickness were performed after embedding in Epon resin and subsequently stained using Ponceau Red or Richardson Blue.

Accession Numbers. Accession numbers of the sequences used for probe synthesis are as follows: *FGF1/2* (EU606032.1), *FGF8/17/18* (EU606035.1), *FGF9/16/20* (EU606036.1), *FGFA* (EU606033.1), *FGFB* (EU606034.1), *FGFC* (EU606038.1), *FGFD* (HM854710), *FGFE* (EU606037.1), *FGFR* (HM854709), *Snail* (HM359129), and *Delta* (HM359124).

1. Letunic I, Doerks T, Bork P (2009) SMART 6: Recent updates and new developments. *Nucleic Acids Res* 37(Database issue):D229–D232.
2. Schultz J, Milpetz F, Bork P, Ponting CP (1998) SMART, a simple modular architecture research tool: Identification of signaling domains. *Proc Natl Acad Sci USA* 95: 5857–5864.
3. Thompson JD, Gibson TJ, Higgins DG (2002) Multiple sequence alignment using ClustalW and ClustalX. *Curr Protoc Bioinformatics*, Chapter 2:Unit 2.3.
4. Galtier N, Gouy M, Gautier C (1996) SEAVIEW and PHYLO_WIN: Two graphic tools for sequence alignment and molecular phylogeny. *Comput Appl Biosci* 12:543–548.
5. Huelsenbeck JP, Ronquist F (2001) MRBAYES: Bayesian inference of phylogenetic trees. *Bioinformatics* 17:754–755.
6. Ronquist F, Huelsenbeck JP (2003) MrBayes 3: Bayesian phylogenetic inference under mixed models. *Bioinformatics* 19:1572–1574.
7. Yu JK, Meulemans D, McKeown SJ, Bronner-Fraser M (2008) Insights from the amphioxus genome on the origin of vertebrate neural crest. *Genome Res* 18: 1127–1132.
8. Meulemans D, Bronner-Fraser M (2007) Insights from amphioxus into the evolution of vertebrate cartilage. *PLoS ONE* 2:e787.
9. Rascol VL, et al. (2009) CASSIOPE: An expert system for conserved regions searches. *BMC Bioinformatics* 10:284.
10. Stamatakis A, Hoover P, Rougemont J (2008) A rapid bootstrap algorithm for the RAxML Web servers. *Syst Biol* 57:758–771.

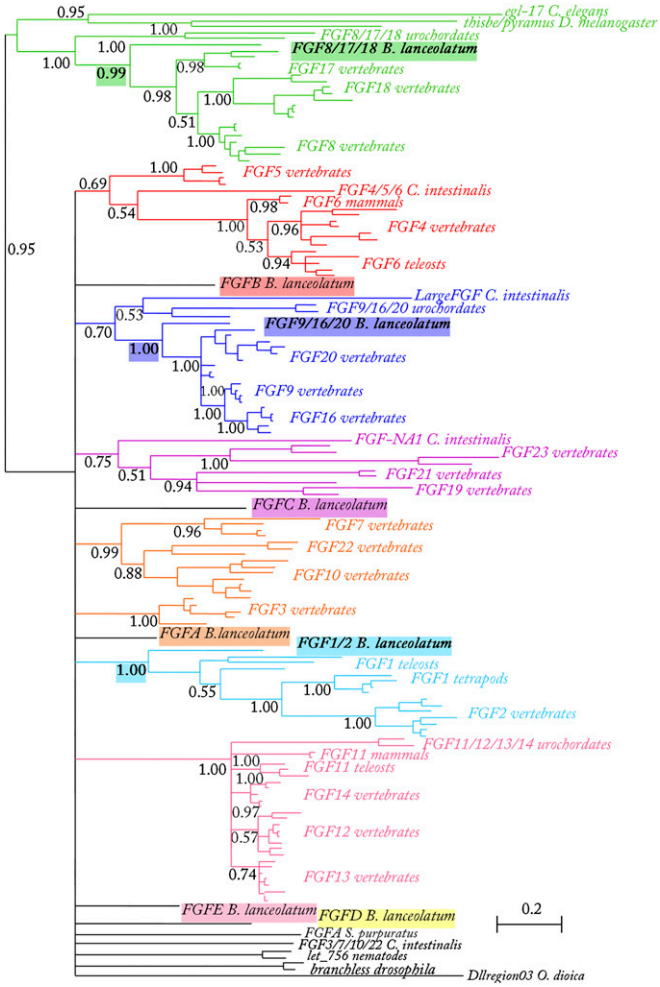

Fig. S1. Phylogenetic analysis of the FGF family. Only FGF domains, as predicted by the online SMART software (http://smart.embl-heidelberg.de/) (1, 2), were used for the alignment. Sequences were aligned automatically using ClustalX (3), with manual correction in Seaview (4). Bayesian inference trees were inferred using MrBayes 3.1.2 (5, 6), with the WAG + G + I model. Two independent runs of 1 million generations each, sampled every 100 generations with two chains, were performed. A 50 majority rule consensus tree was calculated using a 250,000-generation burn-in.

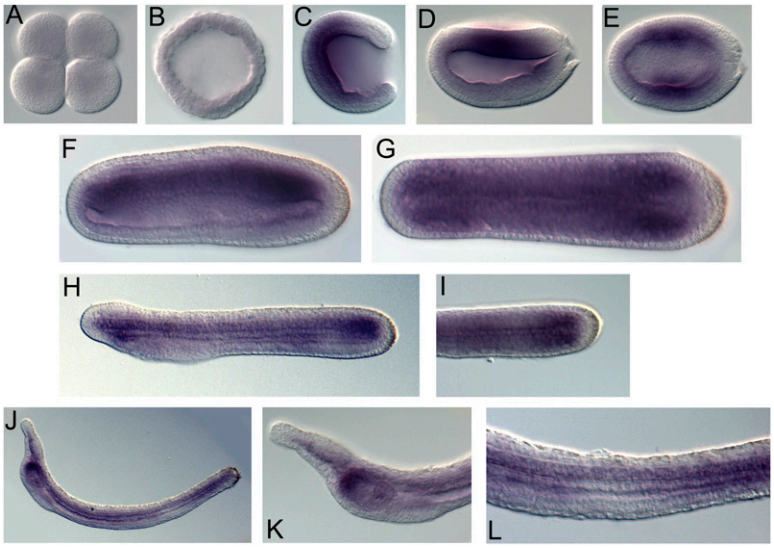

Fig. S2. FGFR expression pattern. The embryos were underincubated in the staining solution to detect the embryonic territories that express FGFR at a higher level. A probe for the TK domain was synthesized (accession no. HM854709). (*A* and *B*) Four-cell and blastula stage embryos showing no or very low expression of FGFR. (*C*) Gastrula stage embryo showing a higher level of expression in the anterior mesendoderm. (*D* and *E*) Lateral and dorsal views of a late gastrula/early neurula stage embryo. At this stage, expression is higher in the paraxial mesoderm. (*F* and *G*) Lateral and dorsal views of a midlate neurula stage embryo showing a higher FGFR expression level in the mesoderm, particularly in the most anterior and posterior somites. (*H*) Late neurula before the mouth opens showing a higher expression level in the notochord, the posterior somites, and the anterior pharyngeal endoderm. (*I*) Dorsal view of the posterior part of the specimen shown in *H*. (*J*) Larva showing a higher expression level in the notochord and the anterior pharyngeal endoderm. In the gut, the iliocolonic region is less strongly labeled than the other regions. (*K*) Enlargement of the anterior part of the specimen shown in *J*. (*L*) Enlargement at the level of the iliocolonic region of the specimen shown in *J*. Side views are shown except when specified. Anterior is to the left, and dorsal is to the top.

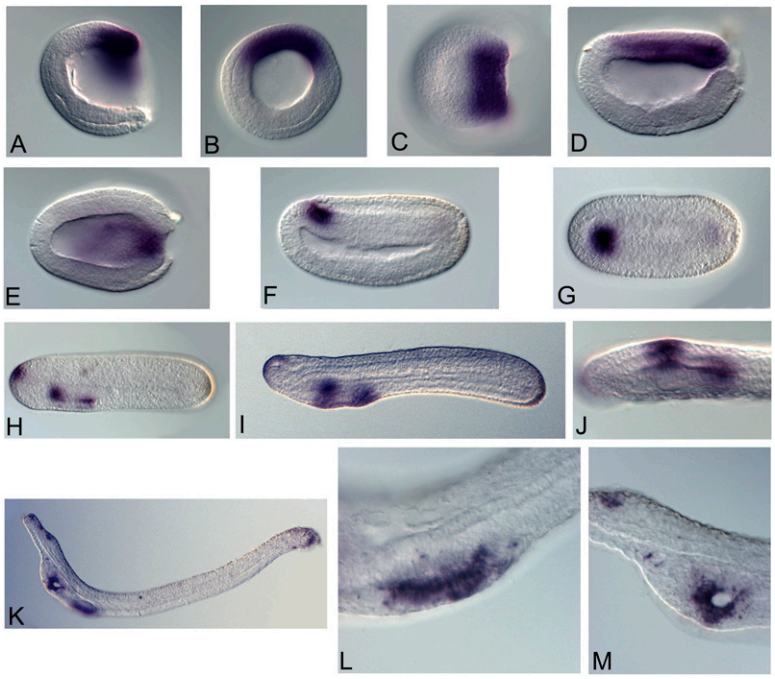

Fig. S3. FGF8/17/18 expression pattern. (*A*–*C*) Lateral, blastopore, and dorsal views of a gastrula stage embryo showing expression in the dorsal posterior mesendoderm. (*D* and *E*) Lateral and dorsal views of a late gastrula/early neurula stage embryo showing expression in the dorsal mesendoderm, with a higher level in the posterior part as described by Yu et al. (7). (*F* and *G*) Lateral and dorsal views of an early midneurula stage embryo showing a very high level of FGF8/17/18 expression in the anterior neural plate and a low level of FGF8/17/18 expression in the posterior mesoderm. (*H*) Lateral view of a midlate neurula stage embryo with expression in the anterior epidermis and in a ventral and a lateral spot in the pharyngeal endoderm as described by Meulemans and Bronner-Fraser (8). (*I*) Late neurula before the mouth opens showing expression in the anterior epidermis and in two regions of the pharyngeal endoderm corresponding to the mouth and first gill slit anlagen. (*J*) Ventral view of the anterior part of the specimen shown in *I*. (*K*) Larva showing expression of FGF8/17/18 in the cerebral vesicle, around the mouth, in the first gill slit, and in the posterior wall of the tailbud. (*L*) Enlargement of the specimen shown in *K* at the level of the first gill slit. (*M*) Enlargement of the specimen shown in *K* at the level of the mouth. Side views are shown except when specified. Anterior is to the left, and dorsal is to the top.

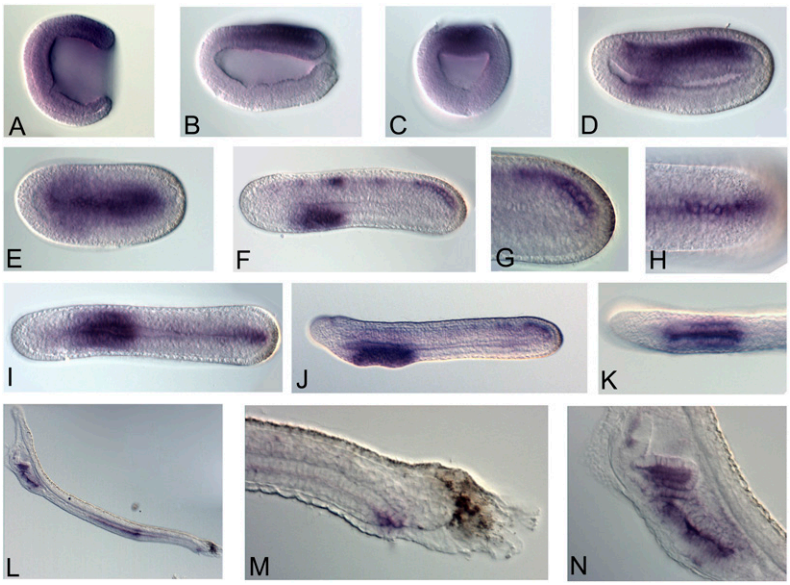

Fig. S4. FGF9/16/20 expression pattern. (*A*) Gastrula stage embryo with a higher level of FGF9/16/20 expression in the posterior dorsal ectoderm. (*B* and *C*) Lateral and blastopore views of a late gastrula stage embryo showing expression in the neural plate. (*D* and *E*) Lateral and dorsal views of an early midneurula stage embryo with labeling in the neural plate and the pharyngeal endoderm. (*F–I*) Views of a midlate neurula embryo. (*F*) Labeling is visible in the neural tube and in the pharyngeal endoderm. (*G*) Enlargement of the posterior part of the embryo shown in *F*. Dorsal view (*I*) and enlargement of the posterior part (*H*). (*J*) Late neurula embryo before the mouth opens showing expression in the pharynx and neural tube. (*K*) Ventral view of the anterior part of the specimen shown in *J*. (*L*) Larva showing FGF9/16/20 expression in the club-shaped gland, the first gill slit, the midgut, and the anus. Enlargement at the level of the tail (*M*) and at the level of the pharynx (*N*) of the larva shown in *L*. Side views are shown except when specified. Anterior is to the left, and dorsal is to the top.

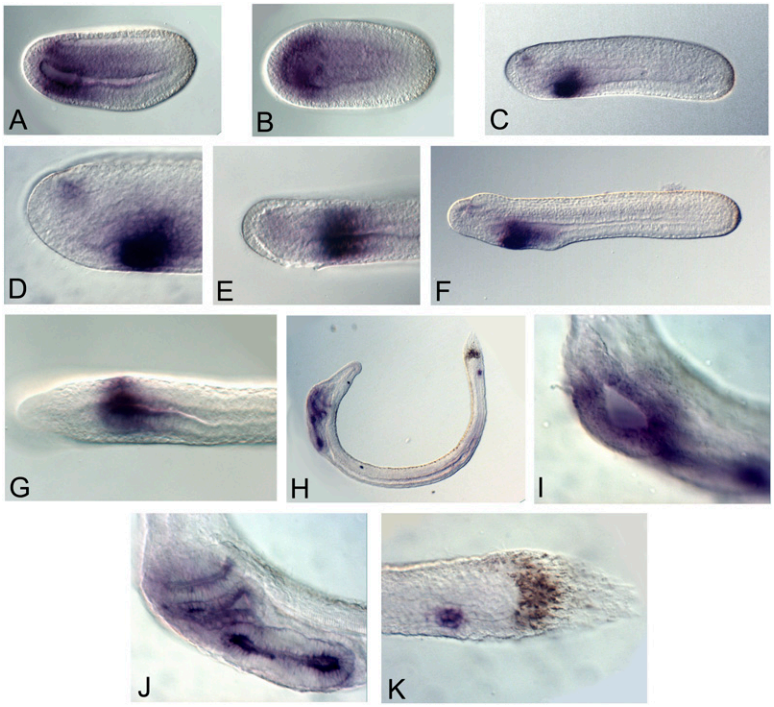

Fig. S5. FGFA expression pattern. (*A* and *B*) Lateral and dorsal views of an early midneurula stage embryo with expression in the anterior neural plate and in the pharyngeal endoderm. (*C*) Midlate neurula stage embryo showing FGFA expression in the cerebral vesicle and the ventral pharyngeal endoderm. (*D* and *E*) Enlarged lateral and ventral views of the specimen shown in *C*. (*F*) Late neurula before the mouth opens with labeling in the cerebral vesicle and in the pharyngeal endoderm. (*G*) Ventral view of the pharyngeal region of the specimen shown in *F*. (*H*) Larva showing FGFA expression around the mouth, in the endostyle, in the club-shaped gland, in the first gill slit, and in the anus. (*I*) Enlargement of the pharyngeal region focused on the mouth. (*J*) Enlargement of the pharyngeal region focusing on the right part. (*K*) Enlargement of the posterior part of the larva shown in *H*. Side views are shown except when specified. Anterior is to the left, and dorsal is to the top.

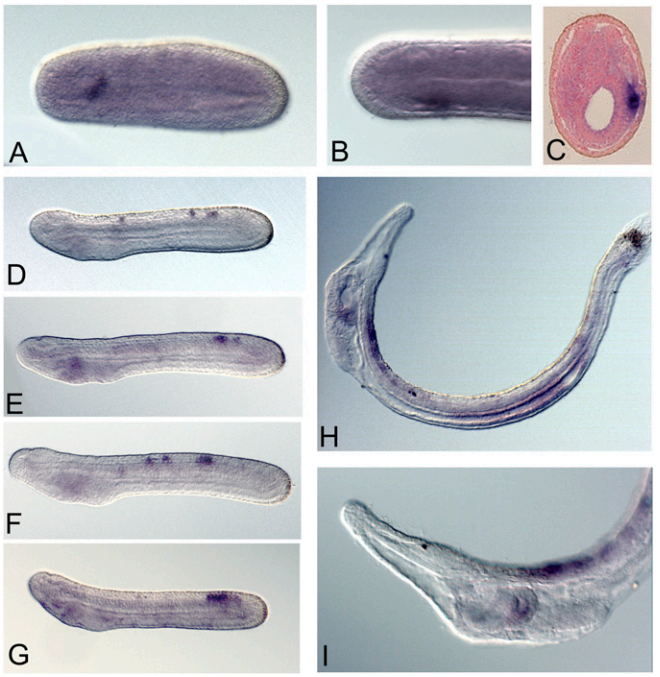

Fig. S6. FGFE expression pattern. (*A*) Midneurula stage embryo with restricted labeling in the first left somite. (*B*) Dorsal view of the anterior region of the specimen in *A*. (*C*) Section of the specimen shown in *A* at the level of the restricted labeling. (*D*–*G*) Late neurula stage embryos before the mouth opens. Dynamic expression is visible in some specific neurons. (*H*) Larva showing expression in the neural tube, the gut, and the club-shaped gland. (*I*) Enlargement of the anterior region of the larva shown in *H*. Side views are shown except when specified. Anterior is to the left, and dorsal is to the top.

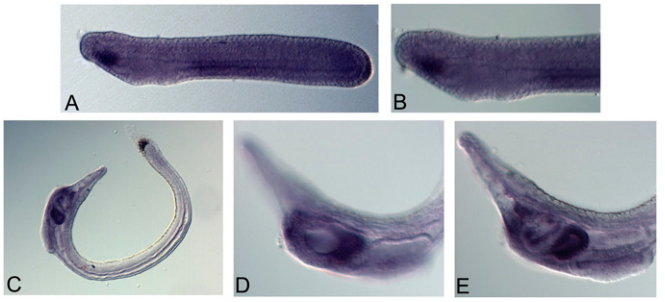

Fig. S7. FGFC expression pattern. (*A*) Late neurula stage embryo showing a higher expression level of FGFC in the anterior pharynx, in the midgut, and in the tailbud. (*B*) Enlargement of the anterior region of the specimen shown in *A*. (*C*) Larva with high FGFC expression level in the club-shaped gland, in the anterior most part of the pharynx, in the preoral pit, and in part of the endostyle. (*D* and *E*) Enlargement of the anterior part of the specimen shown in *C* focused on the mouth and on the right side, respectively. Side views are shown except when specified. Anterior is to the left, and dorsal is to the top.

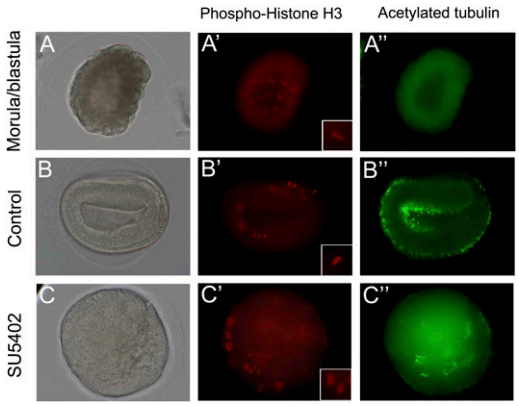

Fig. S8. Embryos treated with SU5402 at the four- to eight-cell stage are not arrested in their development. Immunostaining experiments were performed for WT morula/blastula stage embryos and for embryos treated with SU5402 at the four- to eight-cell stage and fixed at the early midneurula stage, as well as for the corresponding control embryos. In the morula/blastula embryos (*A*), all the cells are dividing, as shown by antiphospho-histone H3 immunostaining (*A′*), but there are still no cilia, as demonstrated by the absence of labeling after antiacetylated-tubulin immunostaining (*A′′*). In the treated embryos (*C*), only some patches of cells are labeled using the antiphospho-histone H3 antibody (*C′*), as in the control embryos (*B*, *B′*). Enlarged images of labeled nuclei are shown at the lower right in *A′*–*C′* (boxes). The antiacetylated-tubulin staining shows that in treated embryos, cilia are well developed (*C′′*), as in control embryos (*B′′*) (*SI Materials and Methods*).

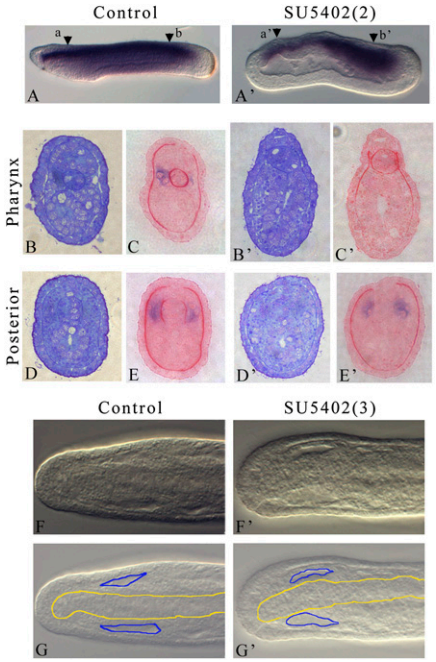

Fig. S9. Somite morphology after treatments with SU5402. (*A*, *A′*) Sections of embryos after in situ hybridization using a probe for *MLC*, stained with Richardson Blue and Ponceau Red. In late neurula stage control embryos, the somites are clearly visible and express *MLC* in the pharyngeal (*B* and *C*, sections at the level of *a* in *A*) and posterior (*D* and *E*, sections at the level of *b* in *A*) regions. In the SU5402-treated (treatment 2; Fig. 3*A*) late neurula stage embryos, no somites are formed in the pharyngeal region (*B′* and *C′*, sections at the level of *a′* in *A′*), whereas in the posterior region, somite morphology and *MLC* expression are normal (*D′* and *E′*, sections at the level of *b′* in *A′*). (*F*, *F′* and *G*, *G′*) differential optic contrast optics images of the anterior part of late neurula stage embryos, dorsal views. The anterior somite cavities are clearly visible in the control embryos (*F* and *G*) as well as in SU5402-treated embryos (treatment 3; Fig. 3*A*) (*F′* and *G′*). (*G*, *G′*) Somite cavities are encircled in yellow and notochord in blue.

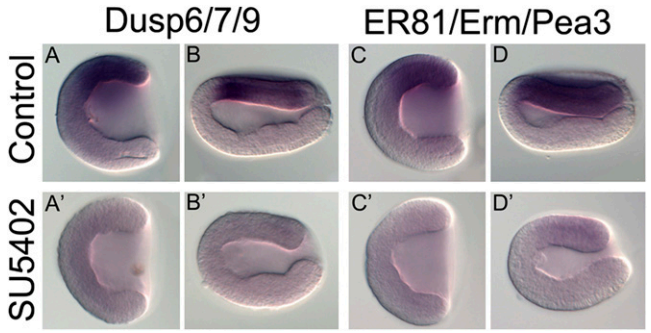

Fig. S10. SU5402 treatment at 50 μM abolishes expression of Dusp6/7/9 and ER81/Erm/Pea3. Embryos were treated from blastula to gastrula or to early neurula stage with 50 μM of SU5402. In situ hybridization experiments were performed using probes for Dusp6/7/9 (HM359125) and ER81/Erm/Pea3 (HM359126) on treated and control embryos. (*A*–*D*) At the gastrula and early neurula stages, Dusp6/7/9 and ER81/Erm/Pea3 are expressed in the dorsal mesendoderm and ectoderm in control embryos. (*A*′–*D*′) In SU5402-treated embryos, expression is totally absent at both stages even after several days of incubation in the staining solution. Dusp6/7/9 and ER81/Erm/Pea3 are the orthologs of well-known FGF pathway target genes in vertebrates. This experiment leads us to suggest, first, that both genes are FGF signaling target genes and, second, that our SU5402 treatment at 50 μM is able to inhibit the pathway completely.

Table S1. Characteristics of eight predicted amphioxus FGF proteins

Name	Protein domain	Exon–intron
Amphioxus FGF1/2	FGF 35–163, 1.86e-44	1–205 // 206–310 // 311–501
Amphioxus FGF8/17/18	Signal peptide 1–31/FGF 55–181, 1.39e-25/low complexity 200–217	1–41 // 42–80 // 81–262 // 263–369 // 370–654
Amphioxus FGF9/16/20	Low complexity 4–19/FGF 48 179, 5.35e-68	1–244 // 245–346 // 347–591
Amphioxus FGFA	Signal peptide 1–16/FGF 56–189, 2.90e-55/low complexity 206–215	1–265 // 266–369 // 370–651
Amphioxus FGFB	Signal peptide 1–24/FGF 55–185, 4.75e-51	1–98 // 99–262 // 263–564
Amphioxus FGFC	Signal peptide 1–20/FGF 60–193, 1.70e-38/low complexity 210–232	1–279 // 280–385 // 386–699
Amphioxus FGFD	Signal peptide 1–26/FGF 51–199, 6.54e-31/low complexity 202–213	1–258 // 259–393 // 394–687
Amphioxus FGFE	FGF 61–192, 9.71e-57	1–283 // 284–386 // 387–582

Protein domains of the eight amphioxus FGFs, predicted by SMART (http://smart.embl-heidelberg.de/), are indicated (including the *e* value for the FGF domain). The exon-intron structure of the coding sequence of the eight amphioxus FGFs is also indicated.

Table S2. Accession number of the genes in the conserved syntenic regions

	Vertebrates paralogues, abbreviations	Vertebrates paralogues, names	*Homo sapiens*	*Monodelphis domestica*	*Canis familiaris*	*Gallus gallus*	*Xenopus tropicalis*	*Tetraodon nigroviridis*	*Proorthologname*	*Branchiostoma floridae*
FGF1/2	BBS7	Bardet–Biedl syndrome 7	ENSG00000138686	ENSMODG00000018927	ENSCAFG00000004128	ENSGALG00000011880		ENSTNIG00000013049	BBS7	113523
	GRXCR1	Glutaredoxin, cysteine-rich 1	*ENSG00000215203*	*ENSMODG00000024820*		ENSGALG00000023032		ENSTNIG00000015736	GRXCR1/2	63706
	GRXCR2	Glutaredoxin, cysteine-rich 2	ENSG00000204928	ENSMODG00000023740	ENSCAFG00000023537	ENSGALG00000023774		ENSTNIG00000018212		
	KIAA0141	KIAA0141	ENSG00000081791	ENSMODG00000010456	ENSCAFG00000006236	*TBLASTN*		ENSTNIG00000014206	KIAA0141	117215
	SPATA5	Spermatogenesis-associated 5	ENSG00000145375	ENSMODG00000018895	ENSCAFG00000003988	ENSGALG00000011833	ENSXETG00000001575		SPATA5	63613, 117082
	SPRY1	Sprouty homolog 1	ENSG00000164056	ENSMODG00000018890	ENSCAFG00000003979		ENSXETG00000001573	ENSTNIG00000013064	SPRY	117102
	SPRY2	Sprouty homolog 2								
	SPRY3	Sprouty homolog 3								
	SPRY4	Sprouty homolog 4	ENSG00000187678	ENSMODG00000023756	ENSCAFG00000006250	ENSGALG00000007336	ENSXETG00000019568	ENSTNIG00000018206		
FGF3/7/10/22	C19orf29	Uncharacterized protein C19orf29 (renal carcinoma antigen NY-REN-24) (cactin)	ENSG00000105298	ENSMODG00000006837	ENSCAFG00000019208				C19orf29	121714
	LMNA	Lamin A/C				ENSGALG00000006083			Nuclear Lamin	121709
	LMNB1	Lamin B1	*ENSG00000113368*			*ENSGALG00000006083*				
	LMNB2	Lamin B2	ENSG00000176619	ENSMODG00000004824	ENSCAFG00000019389	ENSGALG00000000470				
	PIAS1	Protein inhibitor of activated STAT, 1	ENSG00000033800		*ENSCAFG00000017463*	*ENSGALG00000007970*		ENSTNIG00000009549	PIAS1/2/3/4	194147, 279826
	PIAS2	Protein inhibitor of activated STAT, 2				*ENSGALG00000001843*				
	PIAS3	Protein inhibitor of activated STAT, 3								
	PIAS4	Protein inhibitor of activated STAT, 4	ENSG00000105229	*ENSMODG00000000765*	ENSCAFG00000019154	ENSGALG00000001836		ENSTNIG00000003243		

Table S2. Cont.

	Vertebrates paralogues, abbreviations	Vertebrates paralogues, names	*Homo sapiens*	*Monodelphis domestica*	*Canis familiaris*	*Gallus gallus*	*Xenopus tropicalis*	*Tetraodon nigroviridis*	*Proortholog name*	*Branchiostoma floridae*
FGF4/5/6	C12orf4	Uncharacterized protein C12orf4	ENSG00000047621	ENSMODG00000018299	ENSCAFG00000015354	ENSGALG00000017289	ENSXETG00000005966	ENSTNIG00000008813	C12orf4	126642, 283171
	CD9	CD9 molecule	ENSG00000010278	ENSMODG00000018053	ENSCAFG00000015172	ENSGALG00000017274		ENSTNIG00000019223, ENSTNIG00000012685	CD9/81/TSPAN2	96598
	CD81	CD81 molecule	*ENSG00000110651*		ENSCAFG00000010121	ENSGALG00000006546		*ENSTNIG00000013678*		
	TSPAN2	Tetraspanin 2								
	FoxM1	Forkhead box M1	ENSG00000111206	ENSMODG00000018349	ENSCAFG00000015642	ENSGALG00000013420		ENSTNIG00000011394	FoxM	232011
	TSPAN4	Tetraspanin 4	*ENSG00000214063*		ENSCAFG00000025574	ENSGALG00000006837			TSPAN4/9/CD53	231999
	TSPAN9	Tetraspanin 9	ENSG00000011105	ENSMODG00000018335	ENSCAFG00000015466	ENSGALG00000014346		ENSTNIG00000019258, ENSTNIG00000012670		
	CD53	CD53 molecule								
FGF8/17/18	CCNJ	Cyclin J	ENSG00000107443		ENSCAFG00000008454	ENSGALG00000006955		ENSTNIG00000004023	CCNJ/JL	93075
	CCNJL	Cyclin J-like	ENSG00000135083	*ENSMODG00000007987*		ENSGALG00000001455		ENSTNIG00000004651		
	GPAM	Glycerol-3-phosphate acyltransferase, mitochondrial	ENSG00000119927	*ENSMODG00000010326*	ENSCAFG00000010868	ENSGALG00000008795			GPAM	126875, 126887
	GPAT2	Glycerol-3-phosphate acyltransferase 2, mitochondrial		*ENSMODG00000008088*						
	HPSE	Heparanase							HPSE1/2	931000
	HPSE2	Heparanase 2	ENSG00000172987	*ENSMODG00000003602*	ENSCAFG00000009386	ENSGALG00000007508				
	PEBP4	Phosphatidylethanolamine-binding protein 4	ENSG00000134020	ENSMODG00000009235	ENSCAFG00000009270				PEBP4	126894
	RHOBTB1	Rho-related BTB domain containing 1	*ENSG00000072422*	ENSMODG00000017097	*ENSCAFG00000012932*	*ENSGALG00000003073*			RHOBTB1/2	93088
	RHOBTB2	Rho-related BTB domain containing 2	ENSG00000008853	ENSMODG00000009229	ENSCAFG00000009245					

Table S2. Cont.

	Vertebrates paralogues, abbreviations	Vertebrates paralogues, names	*Homo sapiens*	*Monodelphis domestica*	*Canis familiaris*	*Gallus gallus*	*Xenopus tropicalis*	*Tetraodon nigroviridis*	*Proortholog name*	*Branchiostoma floridae*
FGF19/21/23	BANF1	Barrier to autointegration factor 1	ENSG00000175334	ENSMODG00000024907	ENSCAFG00000013083				BANF1/2	202557
	BANF2	Barrier to autointegration factor 2								
	BRMS1	Breast cancer metastasis suppressor 1	ENSG00000174744		ENSCAFG00000012784				BRMS1/1L	260440
	BRMS1L	Breast cancer metastasis-suppressor 1-like				*ENSGALG00000010093*				
	DEDD	Death effector domain containing							DEDD1/2	202645
	DEDD2	Death effector domain containing 2	ENSG00000160570		ENSCAFG00000004892					
	FKBP2	FK506 binding protein 2, 13kDa	ENSG00000173486		ENSCAFG00000014572				FKBP2	83341, 123439
	KAT5	K(lysine) acetyltransferase 5	ENSG00000172977		ENSCAFG00000013299				KAT5	260467
	POU2F1	POU class 2 homeobox 1				*ENSGALG00000015446*			POU2F1/2/3	117908
	POU2F2	POU class 2 homeobox 2	ENSG00000028277		ENSCAFG00000004911					
	POU2F3	POU class 2 homeobox 3	*ENSG00000137709*							
	QPCT	Glutaminyl-peptide cyclotransferase							QPCT/L	275883
	QPCTL	Glutaminyl-peptide cyclotransferase-like	ENSG00000011478		ENSCAFG00000004398					
	SYMPK	Symplekin	ENSG00000125755		ENSCAFG00000004376, ENSCAFG00000023839				SYMPK	202268

Table S2. Cont.

	Vertebrates paralogues, abbreviations	Vertebrates paralogues, names	*Homo sapiens*	*Monodelphis domestica*	*Canis familiaris*	*Gallus gallus*	*Xenopus tropicalis*	*Tetraodon nigroviridis*	*Proortholog name*	*Branchiostoma floridae*
FGFR1/2/3/4	KIAA0232	KIAA0232	ENSG00000170871	ENSMODG00000002906	ENSCAFG00000014342	ENSGALG00000015538			KIAA0232	84842
	PSTK	Phosphoseryl-tRNA kinase	ENSG00000179988	ENSMODG00000007808	ENSCAFG00000012641	ENSGALG00000009610			PSTK	84877
	RGS10	Regulator of G protein signaling 10	ENSG00000148908	ENSMODG00000008876	ENSCAFG00000023428	ENSGALG00000009422			RGS10/12/14	84869
	RGS12	Regulator of G protein signaling 12	ENSG00000159788	ENSMODG00000003502	ENSCAFG00000014641, ENSCAFG00000023428	ENSGALG00000015626				
	RGS14	Regulator of G protein signaling 14	ENSG00000169220	ENSMODG00000004413	ENSCAFG00000016425					
	TMED4	Transmembrane emp24 protein transport domain containing 4							TMED4/9/11	124027
	TMED9	Transmembrane emp24 protein transport domain containing 9	ENSG00000184840	ENSMODG00000004337						
	TMED11	Transmembrane emp24 protein transport domain containing gene		ENSMODG00000004399		ENSGALG00000015722				

The abbreviations and names, as well as the accession numbers, for Homo sapiens, Monodelphis domestica, Canis familiaris, Gallus gallus, Xenopus tropicalis, and Tetraodon nigroviridis are according to the Ensembl database (http://www.ensembl.org). The accession numbers for Branchiostoma floridae genes are according to the JGI amphioxus genome v1.0 (http://genome.jgi-psf.org/Brafl1/Brafl1.home.html). The accession numbers are given only if the genes are in the conserved syntenic region and they are italicized if they are at more than 10 kb from the FGF or FGFR genes of each region.